



**KENNESAW STATE  
UNIVERSITY**

**ADVANCED ELECTRICAL & COMPUTER ENGINEERING**

UNIVERSITY OF KENNESAW

DEPARTMENT OF ELECTRICAL AND COMPUTER ENGINEERING

---

## **Project 1: MIMO-GPR Virtual Array Synthesis**

---

*Authors:*

Student 1 (Hossein Molhem)

Student 2 (ID: your id number)

Date: January 4, 2026

## Contents

<b>1 Project Proposal: MIMO-GPR Virtual Array Synthesis</b>	<b>4</b>
<b>2 Introduction: Major Factors Influencing MIMO System Performance</b>	<b>6</b>
<b>3 Core Physical Principle: The Phase Center Theorem</b>	<b>8</b>
3.1 Bistatic to Monostatic Equivalence . . . . .	8
3.2 Far-Field Approximation . . . . .	8
3.3 Virtual Phase Center . . . . .	8
<b>4 Array Geometry Fundamentals</b>	<b>8</b>
4.1 Physical Array Configuration . . . . .	8
4.2 Virtual Array Synthesis . . . . .	9
<b>5 Linear Array Geometry (1D Case)</b>	<b>9</b>
5.1 Linear Array Case (1D) . . . . .	9
5.2 Virtual Element Positions . . . . .	9
5.3 Aperture Definitions . . . . .	10
5.4 Aperture Expansion Ratio . . . . .	10
<b>6 Linear Array Geometry (1D Case)</b>	<b>10</b>
<b>7 Array Topology Classification</b>	<b>10</b>
7.1 Uniform Linear Array (ULA) . . . . .	10
7.2 Minimum Redundancy Arrays (MRA) . . . . .	11
7.3 Co-Prime Array . . . . .	11
7.4 Nested Array . . . . .	11
<b>8 Redundancy Analysis</b>	<b>12</b>
8.1 Redundancy Matrix . . . . .	12
8.2 Redundancy Count . . . . .	12
<b>9 Redundancy Metrics</b>	<b>12</b>
<b>10 2D Array Geometry</b>	<b>13</b>
10.1 Planar Array Configuration . . . . .	13
10.2 Aperture Area . . . . .	13
10.3 Point Spread Function . . . . .	13
<b>11 Resolution Analysis</b>	<b>14</b>
11.1 Rayleigh Resolution Criterion . . . . .	14
11.2 Resolution Improvement Factor . . . . .	14
11.3 Beamwidth Calculation . . . . .	14

11.4 Grating Lobes Condition . . . . .	15
<b>12 Element Count Relationships</b>	<b>15</b>
12.1 Virtual Element Count . . . . .	15
12.2 Unique Virtual Element Count . . . . .	15
<b>13 Geometric Optimization Criteria</b>	<b>16</b>
13.1 Maximize Virtual Aperture . . . . .	16
13.2 Minimize Redundancy . . . . .	16
13.3 Maximize Unique Virtual Elements . . . . .	16
<b>14 Array Performance Metrics</b>	<b>16</b>
14.1 Geometric Gain . . . . .	17
14.2 Fill Factor . . . . .	17
14.3 Uniformity Index . . . . .	17
<b>15 Implementation Considerations</b>	<b>17</b>
15.1 Computational Complexity . . . . .	17
15.2 Numerical Precision . . . . .	18
15.3 Memory Requirements . . . . .	18
<b>16 Numerical example 1:</b>	<b>18</b>

# 1 Project Proposal: MIMO-GPR Virtual Array Synthesis

This project serves as the first milestone in bridging Geophysics and Data Science. It will be demonstrated how a dense "virtual" array can be mathematically generated using a sparse physical antenna array. This technique is considered fundamental to modern high-resolution Ground-Penetrating Radar (GPR) and seismic imaging in 2026.

## 1. Project Title

Subsurface Resolution Enhancement via MIMO Virtual Array Synthesis

## 2. Objective

To develop a Python-based simulation that calculates the spatial positions of virtual elements in a MIMO (Multiple-Input Multiple-Output) radar system and visualizes the resulting aperture expansion. This allows for higher angular resolution without increasing the number of physical sensors.

## 3. Geophysical Context

In GPR, the ability to resolve two closely spaced objects (like two parallel utility pipes) depends on the size of the array's aperture. Using a MIMO configuration, we create a Virtual Array in which each virtual element represents the effective phase center of a distinct Transmit-Receive (TX-RX) pair.

## 4. Technical Roadmap & Learning Goals

### Phase A: Mathematical Modeling

- **Coordinate Geometry:** Define positions for a set of  $M$  transmitters and  $N$  receivers (e.g., a "Minimum Redundancy Array" or a simple linear sparse layout).
- **Synthesis Algorithm:** Implement the vector addition of TX and RX coordinates. The virtual element position for the  $i$ -th transmitter and  $j$ -th receiver is typically calculated as:

$$POS_{virtual} = \frac{POS_{TX,i} + POS_{RX,j}}{2}$$

- **Redundancy Analysis:** Identify and address overlapping virtual elements that may arise when physical spacing is not optimized.

### Phase B: Data Science Integration (Pandas & Seaborn)

- Data Structuring: Store TX, RX, and Virtual positions in a Pandas DataFrame. Use categorical labeling to distinguish antenna types.
- Seaborn Visualization:
  - Use `sns.scatterplot()` to plot the 1D or 2D array layout.
  - Map the hue and style parameters to the "**Antenna Type**" to clearly visualize the "physical vs. virtual" relationship.
  - Create a "**Density Plot**" of the virtual elements to identify "**effective aperture**" and gaps in the array.

### Phase C: Evaluation Metrics

- **Aperture Gain:** Calculate the ratio of the virtual array length to the physical array length.
- **Resolution Prediction:** Estimate the theoretical angular resolution improvement using the formula  $\theta \approx \lambda/D$ , where  $D$  is the new virtual aperture size.

## 5. Expected Outcomes

- A reusable Python script capable of testing different **MIMO geometries** (e.g., cross-arrays, box arrays, or random sparse arrays).
- High-quality **Seaborn plots** for your portfolio that demonstrate a deep understanding of geophysical signal processing.
- A foundational dataset of virtual positions that will be used in Project 2 (Subsurface Imaging).

## 6. Required Tools (2026 Stack)

- Python 3.12+
- **Pandas:** For managing complex multi-static pairings.
- **Seaborn/Matplotlib:** For high-fidelity geophysical visualization.
- **NumPy:** For vectorized spatial calculations.

## **2 Introduction: Major Factors Influencing MIMO System Performance**

Understanding the performance of a MIMO system requires more than examining its physical configuration or signal model in isolation. MIMO arrays operate at the intersection of geometry, signal characteristics, hardware limitations, algorithmic choices, and system-level design. Each of these dimensions contributes uniquely to the system's ability to resolve targets, suppress interference, maintain robustness, and operate effectively in real environments.

To develop a complete and accurate picture of MIMO performance, it is essential to organize these influences into coherent categories. This structured perspective not only clarifies how different aspects of the system interact, but also highlights where performance gains can be achieved or where degradation may occur.

In this report, the factors governing MIMO performance are grouped into five major categories:

1. Array Geometry,
2. Signal & Source Characteristics,
3. Hardware & Propagation Effects,
4. Algorithmic Factors, and
5. System-Level Parameters.

Together, these categories form a comprehensive framework for analyzing, comparing, and optimizing MIMO systems. By examining each category in depth, we can better understand the fundamental trade-offs, limitations, and opportunities that shape real-world MIMO performance.

**Array Geometry.** Array geometry determines the spatial sampling properties of the MIMO system. The physical and virtual apertures, together with the number and distribution of unique virtual elements, define the achievable angular resolution and sidelobe behavior. Element spacing and array topology (such as ULA, sparse, nested, or co-prime structures) further influence aliasing, coarray completeness, and the effective degrees of freedom.

**Signal & Source Characteristics.** Signal and source characteristics govern how well individual targets or emitters can be separated and estimated. The number of sources relative to the available spatial degrees of freedom, the SNR/INR conditions, and the degree of source coherence strongly affect identifiability and estimation robustness. Bandwidth, number of temporal snapshots, and whether the scenario is far-field or near-field further determine model accuracy and performance limits.

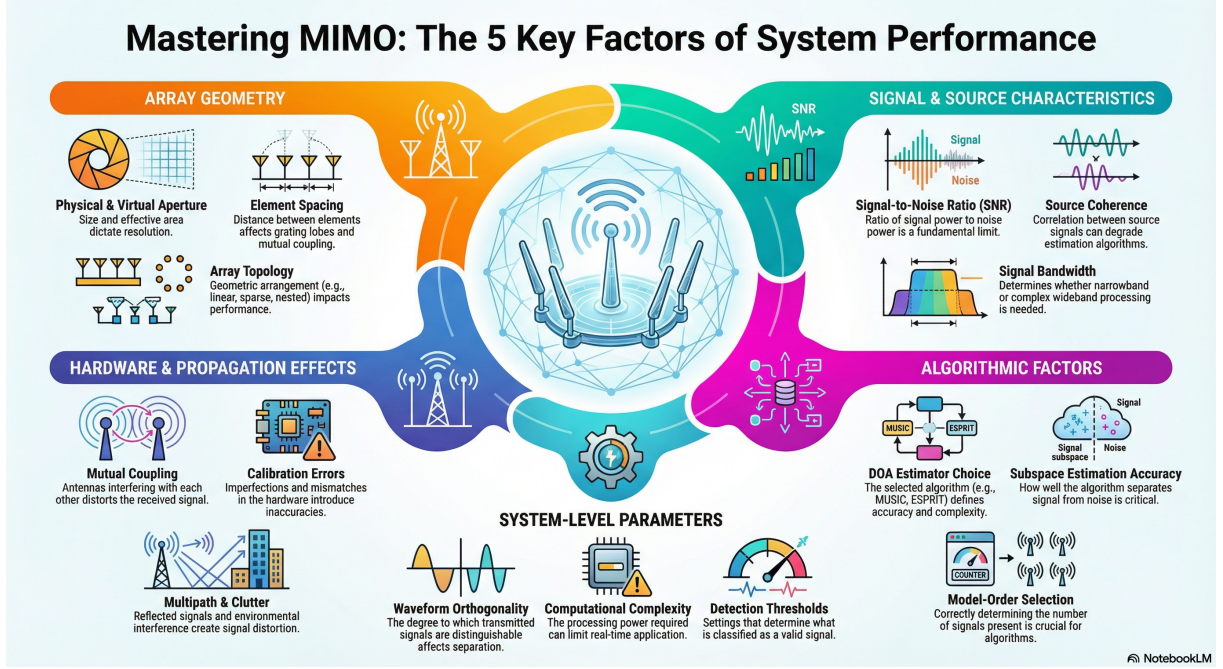


Figure 1

**Hardware & Propagation Effects.** Hardware imperfections and propagation phenomena create discrepancies between the idealized array model and the real system. Mutual coupling, calibration errors, timing and synchronization offsets, phase noise, and RF impairments can distort the received data and introduce bias. In addition, multipath, clutter, and medium-induced distortions impact the effective channel, often requiring compensation or robust processing techniques.

**Algorithmic Factors.** Algorithmic choices dictate how efficiently and accurately the available data are converted into parameter estimates. The selection of DOA estimation method (e.g., MUSIC, ESPRIT, ML, or compressive sensing) determines fundamental trade-offs between resolution, robustness, and complexity. Subspace estimation quality, eigenvalue spread, model-order selection, grid design, and regularization or prior information all influence the estimator's bias, variance, and sensitivity to mismatches.

**System-Level Parameters.** System-level parameters encode how the MIMO configuration is used in practice. Radar mode (monostatic, bistatic, or fully MIMO), waveform orthogonality and coding, PRF, coherent processing interval, and dwell time jointly shape the available diversity and temporal integration. Constraints on computational complexity and latency, together with detection strategies and thresholds (e.g., CFAR or GLRT), ultimately determine the achievable operational performance in realistic scenarios.

## Mathematical Foundation of MIMO-GPR Virtual Array Synthesis

### 3 Core Physical Principle: The Phase Center Theorem

#### 3.1 Bistatic to Monostatic Equivalence

The fundamental concept underpinning virtual array synthesis is the **Effective Phase Center** principle. For a bistatic radar system with transmitter at position  $\mathbf{p}_t$  and receiver at position  $\mathbf{p}_r$ , the round-trip phase to a point target at position  $\mathbf{p}_\tau$  is:

$$\phi = \frac{2\pi}{\lambda} (\|\mathbf{p}_t - \mathbf{p}_\tau\| + \|\mathbf{p}_r - \mathbf{p}_\tau\|) \quad (1)$$

#### 3.2 Far-Field Approximation

For targets in the **far-field** (Fraunhofer region), where  $\|\mathbf{p}_\tau\| \gg \|\mathbf{p}_t\|, \|\mathbf{p}_r\|$ , we can approximate:

$$\phi \approx \frac{4\pi}{\lambda} \left\| \frac{\mathbf{p}_t + \mathbf{p}_r}{2} - \mathbf{p}_\tau \right\| \quad (2)$$

#### 3.3 Virtual Phase Center

This demonstrates that the bistatic pair behaves as a **monostatic radar** located at the midpoint:

$$\mathbf{p}_v = \frac{\mathbf{p}_t + \mathbf{p}_r}{2} \quad (3)$$

## 4 Array Geometry Fundamentals

This section introduces the foundational geometric definitions used in MIMO array analysis. The physical array layout determines the available transmitter and receiver positions, while virtual array synthesis expands these into a richer set of spatial sampling points.

### 4.1 Physical Array Configuration

Let:

- $M$  transmitters at positions:  $\mathbf{P}_T = \{\mathbf{p}_{T,1}, \mathbf{p}_{T,2}, \dots, \mathbf{p}_{T,M}\}$

- $N$  receivers at positions:  $\mathbf{P}_R = \{\mathbf{p}_{R,1}, \mathbf{p}_{R,2}, \dots, \mathbf{p}_{R,N}\}$

The physical array configuration defines the actual hardware layout. These transmitter and receiver coordinates form the basis for constructing the virtual array through pairwise combinations.

## 4.2 Virtual Array Synthesis

The virtual array  $\mathbf{P}_V$  contains  $M \times N$  elements:

$$\mathbf{P}_V = \left\{ \mathbf{p}_{V,ij} = \frac{\mathbf{p}_{T,i} + \mathbf{p}_{R,j}}{2} : i = 1, \dots, M; j = 1, \dots, N \right\} \quad (4)$$

Virtual array synthesis generates a midpoint for every transmitter–receiver pair, effectively expanding the spatial sampling aperture. This virtual geometry enables improved resolution and richer spatial diversity compared to the physical array alone.

# 5 Linear Array Geometry (1D Case)

This section describes the geometry of one-dimensional linear arrays, where all elements lie along the x-axis. The 1D case forms the foundation for understanding virtual array synthesis and aperture expansion in more complex geometries.

## 5.1 Linear Array Case (1D)

For a linear array along the x-axis:

- Transmitters:  $\mathbf{p}_{T,i} = (x_{T,i}, 0)$
- Receivers:  $\mathbf{p}_{R,j} = (x_{R,j}, 0)$

In this configuration, all physical elements share the same vertical coordinate, simplifying the geometry and enabling straightforward virtual position generation.

## 5.2 Virtual Element Positions

The virtual elements become:

$$x_{V,ij} = \frac{x_{T,i} + x_{R,j}}{2}$$

Each transmitter–receiver pair produces a virtual element located at the midpoint of their x-coordinates. This forms the 1D virtual array used for beamforming and resolution enhancement.

### 5.3 Aperture Definitions

Physical Array Aperture:

$$D_p = \max(\max(x_T), \max(x_R)) - \min(\min(x_T), \min(x_R)) \quad (5)$$

Virtual Array Aperture:

$$D_v = \max(x_V) - \min(x_V) \quad (6)$$

The physical aperture represents the span of all physical elements, while the virtual aperture reflects the effective span of the synthesized virtual positions. Typically,  $D_v > D_p$ , enabling improved angular resolution.

### 5.4 Aperture Expansion Ratio

The aperture expansion ratio is:

$$R = \frac{D_v}{D_p} = \frac{\max(x_V) - \min(x_V)}{\max(\max(x_T), \max(x_R)) - \min(\min(x_T), \min(x_R))} \quad (7)$$

This ratio quantifies how much the virtual array expands the effective aperture relative to the physical array. Larger values of  $R$  indicate greater resolution enhancement.

## 6 Linear Array Geometry (1D Case)

This section describes the geometry of one-dimensional linear arrays, where all elements lie along the x-axis. The 1D case forms the foundation for understanding virtual array synthesis and aperture expansion in more complex geometries.

## 7 Array Topology Classification

This section summarizes common array topologies used in MIMO systems. Each topology offers different trade-offs in aperture growth, redundancy, and virtual element diversity, making topology selection a key design decision.

### 7.1 Uniform Linear Array (ULA)

A ULA is the simplest and most widely used array structure, characterized by constant inter-element spacing.

- Equal spacing between adjacent elements
- Spacing typically  $d = \lambda/2$

- Virtual array length:  $D_V = (M + N - 2)d/2$

The ULA provides a fully contiguous virtual coarray but is more susceptible to mutual coupling and offers limited flexibility in redundancy control.

## 7.2 Minimum Redundancy Arrays (MRA)

MRAs are designed to minimize repeated virtual positions while maximizing aperture coverage.

For  $M$  transmitters and  $N$  receivers, the optimal physical spacing minimizes:

$$J = \sum_{x \in \mathcal{X}_V} (r(x) - 1)^2 \quad (8)$$

subject to constraints on total array length.

MRAs achieve the smallest possible redundancy for a given number of elements, producing highly efficient virtual apertures.

## 7.3 Co-Prime Array

Co-prime arrays exploit number-theoretic spacing to generate large virtual apertures with relatively few physical elements.

- Transmitter spacing:  $M$ -element ULA with spacing  $N\lambda/2$
- Receiver spacing:  $N$ -element ULA with spacing  $M\lambda/2$
- Creates  $MN - M - N + 1$  unique virtual elements

This structure yields a sparse but hole-free difference coarray, enabling high-resolution processing with reduced hardware complexity.

## 7.4 Nested Array

Nested arrays combine dense and sparse subarrays to achieve both high resolution and low redundancy.

- Inner ULA with  $N_1$  elements spaced  $d_1 = \lambda/2$
- Outer ULA with  $N_2$  elements spaced  $d_2 = (N_1 + 1)d_1$
- Creates  $N_1 N_2 + N_1 + N_2$  virtual elements

The nested structure produces a fully contiguous virtual coarray with significantly fewer physical elements than a full ULA.

## 8 Redundancy Analysis

This section formalizes how redundancy is quantified in virtual arrays. Redundancy arises when multiple transmitter–receiver pairs generate identical virtual positions, reducing sampling efficiency but also enabling robustness in some configurations.

### 8.1 Redundancy Matrix

Define the redundancy matrix  $\mathbf{R}$  with elements:

$$R_{ij,kl} = \delta(x_{V,ij} - x_{V,kl}) \quad (9)$$

where  $\delta(\cdot)$  is the Kronecker delta.

The redundancy matrix encodes pairwise equality between virtual positions. Each entry indicates whether two virtual elements occupy the same spatial location, forming the basis for redundancy quantification.

### 8.2 Redundancy Count

For virtual position  $x$ , the redundancy count is:

$$r(x) = \sum_{i=1}^M \sum_{j=1}^N \sum_{k=1}^M \sum_{l=1}^N \delta(x_{V,ij} - x) \delta(x_{V,kl} - x) \quad (10)$$

The redundancy count  $r(x)$  measures how many times a specific virtual position is generated across all transmitter–receiver combinations. Higher values indicate repeated sampling of the same location, reducing the number of unique virtual elements.

## 9 Redundancy Metrics

This section defines two key metrics used to quantify how efficiently a MIMO array converts physical elements into distinct virtual sampling positions. These measures help assess coarray quality, spatial diversity, and geometric efficiency.

**Redundancy Ratio:**

$$\rho = \frac{\text{Total Virtual Elements}}{\text{Unique Virtual Elements}} \quad (11)$$

The redundancy ratio  $\rho$  measures how many virtual positions are duplicated on average. A value close to 1 indicates minimal redundancy, while larger values imply repeated virtual positions and reduced sampling efficiency.

**Array Efficiency:**

$$\eta = \frac{\text{Unique Virtual Elements}}{\text{Physical Elements}} \quad (12)$$

Array efficiency  $\eta$  quantifies how effectively the physical array generates distinct virtual positions. Higher efficiency reflects better geometric expansion and improved spatial resolution potential.

## 10 2D Array Geometry

This section extends the virtual array formulation to two-dimensional (planar) configurations. By incorporating both  $x$ - and  $y$ -coordinates, 2D arrays enable improved angular resolution, full azimuth–elevation coverage, and more flexible aperture shaping.

### 10.1 Planar Array Configuration

For 2D arrays with coordinates  $(x, y)$ , the virtual array position vector is defined as:

$$\mathbf{p}_{V,ij} = \left( \frac{x_{T,i} + x_{R,j}}{2}, \frac{y_{T,i} + y_{R,j}}{2} \right) \quad (13)$$

This midpoint formulation synthesizes a virtual element for each transmitter–receiver pair, extending the virtual aperture across both spatial dimensions.

### 10.2 Aperture Area

Physical Array Area:

$$A_P = [\max(x_T, x_R) - \min(x_T, x_R)] \times [\max(y_T, y_R) - \min(y_T, y_R)] \quad (14)$$

Virtual Array Area:

$$A_V = [\max(x_V) - \min(x_V)] \times [\max(y_V) - \min(y_V)] \quad (15)$$

The physical and virtual aperture areas quantify the spatial extent of the array in two dimensions. A larger virtual area generally leads to finer azimuth–elevation resolution and improved imaging capability.

### 10.3 Point Spread Function

The point spread function (PSF) in the spatial frequency domain  $(k_x, k_y)$  is:

$$PSF(k_x, k_y) = \left| \sum_{i=1}^M \sum_{j=1}^N \exp(-j(k_x x_{V,ij} + k_y y_{V,ij})) \right|^2 \quad (16)$$

The PSF characterizes the array's 2D spatial response and determines its ability to localize targets in angle. A well-designed virtual geometry yields a narrow, symmetric mainlobe and suppressed sidelobes in both dimensions.

## 11 Resolution Analysis

This section presents key resolution metrics for physical and virtual arrays, including Rayleigh-based limits, improvement factors, beamwidth expressions, and grating-lobe constraints. These relationships quantify how virtual aperture expansion enhances angular resolution.

### 11.1 Rayleigh Resolution Criterion

Physical Array Resolution:

$$\Delta\theta_P = \frac{\lambda}{2D_P \cos \theta_0} \quad (17)$$

Virtual Array Resolution:

$$\Delta\theta_V = \frac{\lambda}{2D_V \cos \theta_0} \quad (18)$$

The Rayleigh criterion provides a fundamental limit on angular resolution. Increasing the aperture from  $D_P$  to  $D_V$  directly reduces the minimum resolvable angle.

### 11.2 Resolution Improvement Factor

The resolution improvement factor is:

$$F = \frac{\Delta\theta_P}{\Delta\theta_V} = \frac{D_V}{D_P} \quad (19)$$

This factor quantifies how much the virtual array improves resolution relative to the physical array. A larger virtual aperture yields proportionally finer angular discrimination.

### 11.3 Beamwidth Calculation

The array factor for the virtual array is:

$$AF(\theta) = \sum_{m=1}^M \sum_{n=1}^N w_{mn} \exp\left(-j \frac{4\pi}{\lambda} x_{V,mn} \sin \theta\right) \quad (20)$$

The half-power beamwidth is approximately:

$$\theta_{BW} \approx 0.886 \frac{\lambda}{2D_V \cos \theta_0} \quad [\text{radians}] \quad (21)$$

Beamwidth provides a practical measure of angular selectivity. A larger virtual aperture narrows the mainlobe, improving target separation.

## 11.4 Grating Lobes Condition

Avoid grating lobes when:

$$|d_{\text{eff}}| \leq \frac{\lambda}{2 \sin \theta_{\max}} \quad (22)$$

Here,  $d_{\text{eff}}$  is the effective spacing between virtual elements. This condition ensures that no secondary lobes appear within the visible region, preserving unambiguous angular estimation.

# 12 Element Count Relationships

This section summarizes the fundamental relationships between physical elements, total virtual elements, and unique virtual elements in a MIMO array. These relationships help quantify how efficiently the array geometry converts physical hardware into spatial sampling capability.

$$N_V = M \times N \quad (23)$$

The total number of virtual elements  $N_V$  is obtained by pairing every transmitter with every receiver. This represents the full set of Tx–Rx combinations before accounting for redundancy.

## 12.1 Virtual Element Count

For optimal arrays:

$$|N_{V,\text{unique}}| \approx \frac{MN}{2} \quad (\text{for well-designed arrays}) \quad (24)$$

The number of unique virtual elements reflects how many distinct spatial positions are synthesized. In well-designed sparse or co-prime arrays, approximately half of the total virtual combinations produce unique positions, reducing redundancy while maintaining aperture growth.

## 12.2 Unique Virtual Element Count

$$\alpha = \frac{N_V}{M + N} \quad (25)$$

The element multiplication factor  $\alpha$  measures how many virtual elements are generated per physical element. Higher values indicate more efficient spatial expansion, while lower values suggest redundancy or limited geometric diversity.

## 13 Geometric Optimization Criteria

This section outlines three core objectives for optimizing virtual array geometry: maximizing aperture span, minimizing redundancy, and maximizing the number of unique virtual positions. These criteria directly impact resolution, sampling efficiency, and coarray completeness.

### 13.1 Maximize Virtual Aperture

$$\max D_V = \max(x_V) - \min(x_V) \quad (26)$$

$$\text{subject to: } x_{T,i} \in [0, L_T], \quad x_{R,j} \in [0, L_R] \quad (27)$$

Maximizing the virtual aperture  $D_V$  increases angular resolution and spatial coverage. The constraint ensures transmitter and receiver positions remain within their physical bounds.

### 13.2 Minimize Redundancy

$$\min \sum_{x \in \mathcal{X}_V} (r(x) - 1)^2 \quad (28)$$

This objective penalizes repeated virtual positions, promoting a more uniform and efficient sampling of the aperture. The redundancy count  $r(x)$  reflects how many times each virtual position is synthesized.

### 13.3 Maximize Unique Virtual Elements

$$\max |\mathcal{X}_V| \quad (29)$$

Maximizing the cardinality of  $\mathcal{X}_V$ , the set of unique virtual positions, enhances spatial diversity and coarray completeness. A larger unique set improves resolution and reduces ambiguity.

## 14 Array Performance Metrics

This section defines key metrics used to evaluate the spatial efficiency and sampling quality of MIMO arrays. These metrics quantify geometric expansion, sampling density, and distribution uniformity of virtual elements.

## 14.1 Geometric Gain

$$G_{\text{geom}} = \frac{D_V}{D_P} \times \frac{N_{V,\text{unique}}}{M + N} \quad (30)$$

Geometric gain measures the normalized aperture expansion and virtual sampling efficiency relative to the physical array. Here,  $D_V$  and  $D_P$  denote the virtual and physical aperture spans, respectively, and  $N_{V,\text{unique}}$  is the number of unique virtual elements.

## 14.2 Fill Factor

$$F = \frac{N_{V,\text{unique}}}{D_V/d_{\min}} \quad (31)$$

The fill factor quantifies how densely the virtual aperture is populated relative to the minimum required spacing  $d_{\min}$ . A value close to 1 indicates efficient spatial utilization without excessive redundancy.

## 14.3 Uniformity Index

$$U = 1 - \frac{\sigma_d}{\bar{d}} \quad (32)$$

The uniformity index captures the regularity of virtual element spacing. Here,  $\sigma_d$  is the standard deviation and  $\bar{d}$  is the mean spacing between adjacent virtual elements. A value near 1 indicates highly uniform spacing, while lower values suggest irregular or clustered distributions.

# 15 Implementation Considerations

This section outlines practical aspects of implementing virtual array systems, including computational complexity, numerical precision, and memory requirements.

## 15.1 Computational Complexity

- Virtual array generation:  $O(MN)$
- Redundancy analysis (naive):  $O((MN)^2)$
- Optimized algorithms:  $O(MN \log(MN))$

These complexities reflect the cost of generating virtual positions and analyzing redundancy. Efficient implementations can significantly reduce runtime for large arrays.

## 15.2 Numerical Precision

$$\phi_{ij} = \mod\left(\frac{4\pi}{\lambda}x_{V,ij}\sin\theta, 2\pi\right) \quad (33)$$

Phase calculations require careful handling of modulo operations to ensure numerical stability, especially when dealing with high-resolution virtual positions and small wavelengths.

## 15.3 Memory Requirements

$$\text{Memory} \approx 8 \times M \times N \text{ bytes (double precision)} \quad (34)$$

Memory usage scales linearly with the number of virtual elements. For double-precision storage, each element requires 8 bytes, making memory efficiency critical for large-scale systems.

# 16 Numerical example 1:

## Problem Statement

Consider a sparse  $2 \times 2$  MIMO array configuration ( $M = 2, N = 2$ ) with the following physical coordinates (in meters):

- **Transmitters ( $T$ ):** Locations at 0.0 m and 0.6 m.
  - **Receivers ( $R$ ):** Locations at 0.2 m and 0.8 m.
  - **Frequency ( $f$ ):** 500 MHz ( $c = 3 \times 10^8$  m/s).
1. **Calculate the Wavelength ( $\lambda$ ):** Determine the signal wavelength in free space.
  2. **Synthesize the Virtual Array:** Calculate the position of all 4 virtual elements ( $p_{v,11}, p_{v,12}, p_{v,21}, p_{v,22}$ ).
  3. **Analyze Redundancy:** Identify if any virtual elements overlap. How many unique spatial sampling points does this array provide?
  4. **Compare Apertures:** Calculate the Physical Aperture width ( $D_{\text{phys}}$ ) and the synthesized Virtual Aperture width ( $D_{\text{virt}}$ ). What is the Aperture Gain?
  5. **Evaluate Resolution Improvement:** Compute the theoretical angular resolution for both the physical and virtual arrays. By what factor does the MIMO configuration improve the resolution?

## Solution

**calculate the Wavelength  $\lambda$ :**

$$\lambda = \frac{c}{f} = \frac{3 \times 10^8}{500 \times 10^6} = 0.6$$

**Synthesize the Virtual Array:**

- **Transmitters ( $M = 2$ ):** Vector of positions

$$\mathbf{P}_T = \{\mathbf{p}_{T,1}, \mathbf{p}_{T,2}\} = \{0.0, 0.6\} \text{ m}$$

- **Receivers ( $N = 2$ ):** Vector of positions

$$\mathbf{P}_R = \{\mathbf{p}_{R,1}, \mathbf{p}_{R,2}\} = \{0.2, 0.8\} \text{ m}$$

According to (4), the virtual array contains  $M \times N = 2 \times 2 = 4$  elements, and its vector is given by:

$$\begin{aligned} \mathbf{P}_V &= \left\{ \mathbf{p}_{V,ij} = \frac{\mathbf{p}_{T,i} + \mathbf{p}_{R,j}}{2} : i = 1, 2; j = 1, 2 \right\} \\ &= \{\mathbf{p}_{V,11}, \mathbf{p}_{V,12}, \mathbf{p}_{V,21}, \mathbf{p}_{V,22}\} \\ &= \left\{ \frac{\mathbf{p}_{T,1} + \mathbf{p}_{R,1}}{2}, \frac{\mathbf{p}_{T,1} + \mathbf{p}_{R,2}}{2}, \frac{\mathbf{p}_{T,2} + \mathbf{p}_{R,1}}{2}, \frac{\mathbf{p}_{T,2} + \mathbf{p}_{R,2}}{2} \right\} \\ &= \left\{ \frac{0.0 + 0.2}{2}, \frac{0.0 + 0.8}{2}, \frac{0.6 + 0.2}{2}, \frac{0.6 + 0.8}{2} \right\} \\ &= \{0.1, 0.4, 0.4, 0.7\} \end{aligned}$$

**Analyze Redundancy:**

virtual array vector is

$$\mathbf{P}_V = [0.1 \ 0.4 \ 0.4 \ 0.7]$$

Unique virtual positions:

$$\mathbf{P}_V = [0.1 \ 0.4 \ 0.7]$$

Total virtual elements: 4

Number of unique elements: 3

Redundancy: 1 duplicated element

as result:

The virtual array contains 4 elements, of which 3 are unique. The unique virtual positions are [0.1, 0.4, 0.7], indicating that 1 element is duplicated.

**Compare Apertures:**
**Aperture Calculation:**

Physical element positions: [0.0, 0.2, 0.6, 0.8] Minimum position: 0.0 m, Maximum position: 0.8 m Physical aperture:

$$D_{\text{phys}} = 0.8 - 0.0 = 0.8 \text{ m}$$

**Virtual Array:** Virtual element positions: [0.1, 0.4, 0.4, 0.7] Minimum position: 0.1 m, Maximum position: 0.7 m Virtual aperture:

$$D_{\text{virt}} = 0.7 - 0.1 = 0.6 \text{ m}$$

**Aperture Gain:**

$$G = \frac{D_{\text{virt}}}{D_{\text{phys}}} = \frac{0.6}{0.8} = 0.75$$

**Evaluate Resolution Improvement:**

**Wavelength:** Frequency: 500 MHz Speed of light:  $c = 3 \times 10^8 \text{ m/s}$

$$\lambda = \frac{c}{f} = \frac{3 \times 10^8}{5 \times 10^8} = 0.60 \text{ m}$$

**Physical Array Resolution:**

$$\theta_{\text{phys}} = \frac{\lambda}{2D_{\text{phys}}} = \frac{0.60}{2 \times 0.8} = \frac{0.60}{1.6} = 0.375 \text{ rad} \approx 21.49^\circ$$

**Virtual Array Resolution:**

$$\theta_{\text{virt}} = \frac{\lambda}{2D_{\text{virt}}} = \frac{0.60}{2 \times 0.6} = \frac{0.60}{1.2} = 0.50 \text{ rad} \approx 28.65^\circ$$

**Resolution Improvement:**

$$\frac{\theta_{\text{phys}}}{\theta_{\text{virt}}} = \frac{0.375}{0.50} = 0.75$$

**Table 1:** Summary of Array Metrics

Metric	Value
Physical Aperture	0.800 m
Virtual Aperture	0.600 m
Aperture Gain	0.75
Physical Resolution	21.49°
Virtual Resolution	28.65°
Resolution Improvement	0.75×
Physical Elements	4
Virtual Elements	4
Element Multiplication	1.0×

## References